Biomass Conversion and Biorefinery
https://doi.org/10.1007/s13399-023-04475-4

ORIGINAL ARTICLE

Recycling textile waste into innovative carbon black and applications to smart textiles: a sustainable approach

Aamer Khan[1] · **Muhammad Awais**[1] · **Muhammad Mohsin**[1]

Received: 16 March 2023 / Revised: 5 June 2023 / Accepted: 6 June 2023

Abstract

In this study, carbon black was synthesized by the utilization of synthetic textile waste (waste polyester fabric (PET) and polyester cotton (50:50) blend (PC)) in a horizontal tube furnace in a temperature range of 700~1000 °C keeping the heating rate at a uniform 5 °C/min in nitrogen environment. The market for environmentally friendly conductive inks for textile printing is unfilled, but our study fills that void. Using synthetic textile scraps as a replacement for fossil fuels in the carbon black manufacturing process is an innovative and environmentally friendly way to lessen the number of textiles that end up in landfills. This process of producing conductive inks has several potential uses. Some examples include electrical textiles, smart textiles, and wearable technologies. The morphology and structure of the obtained carbon black were studied via scanning electron microscopy and Raman spectroscopy and compared with the commercial carbon black (CCB). PC-based carbon black exhibited superior structural properties, while PET-based carbon black exhibited comparable properties to the CCB. The lab grown carbon black is approximately 50% cheaper than the commercial carbon black. Conductive inks were manufactured using the obtained carbon black and commercial carbon black. Screen printing was carried out using different conductive inks on 100% cotton fabric substrate. Conductivity measurements revealed that lab grown carbon black based on PC exhibited 6.1% more conductivity than the commercial carbon black, while the one based on 100% polyester waste fabric depicted comparable conductivity to the commercial carbon black-based ink and remained stable until 10 washes. The lab grown carbon black printed fabrics also exhibited comparable tensile strength, tear strength, flexural rigidity, air permeability, and crocking fastness (dry and wet) tests to the commercial carbon black. The printed patches were stable and did not affect the wearability performances of the fabric after the printing of conductive inks. Based on the obtained results, it can be safely concluded that waste synthetic textile materials can serve as an alternative precursor for the synthesis of commercial carbon black and subsequent applications in smart textiles.

Keywords Carbon black · Recycling · Textile waste · Pyrolysis · Sustainability · Smart textiles

1 Introduction

The demand for textile products is increasing day by day due to population growth and improved living standards [1]. Textile consumption is expected to increase three times by 2050 globally compared to 2015 [2]. The textile sector is the fifth largest pollution-contributing sector worldwide and accounts for 3% of all greenhouse gas emissions [3, 4]. According to an international survey, more than 110 million tons of apparel and textile fibers are produced annually around the world, which in turn leads to the generation of a huge amount of textile waste [5]. Most of the textile waste is disposed of by incineration and in landfills as municipal solid waste [6] which creates environmental and economic crises [7]. Environmental crises are represented in the form of pollution and the emission of hazardous gases, while the economic consequences are shown in the form of the amount of land consumed in landfills [8]. For this reason, scientists are rushing to overcome these consequences by reusing and or recycling textile waste, reducing carbon emissions by burning them, and at the same time also trying to preserve the environment [9]. The textile industry is contributing to a huge environmental crisis due to the usage of a huge percentage of synthetic fibers derived from fossil fuels [10]. Around 63% of textile fibers

✉ Aamer Khan
aamir.abbas@uet.edu.pk

[1] Department of Textile Engineering, University of Engineering and Technology Lahore (Faisalabad campus), Lahore 38000, Pakistan

Published online: 14 June 2023

used today come from petrochemical sources, and polyester is the most commonly used fiber. Fossil fuels already account for over 80% of energy use, contributing to climate change, global warming, and the rapid depletion of natural energy supplies. The overuse of oil, gas, and coal increases the demand for these resources, which could lead to pollution that threatens water and oxygen supplies [11, 12]. The global market size of polyester was more than 90 billion dollars in 2020 and is expected to grow at a cumulative annual growth rate of 7.8% from 2021 to 2027 due to the rising demand for polyester fiber in the textile industry and other application areas as well [13–15]. Cotton is a cellulose-based polymer that is predominantly used to make clothing (about 70%), household textiles (about 35%), and industrial goods (the remaining 5%). Cotton agriculture has a significant effect on water usage, contributing to drought with its 2.6% share of global water use. In addition, the use of fuels or energy-intensive material inputs, such as fertilizers, herbicides, seeds, diesel fuel, and electricity for irrigation, machinery, and labor, makes cotton cultivation a major contributor to greenhouse gases, accounting for between 0.3 and 1% of total global warming potential [16–25]. According to the research, around 10% of world carbon emissions are generated by the textile sector [26]. The remaining 37% of natural fibers are used in industries, but they consume a huge amount of water associated with water depletion and toxic pollution caused by intensive use of pesticides [27]. The textile and clothing industries are responsible for more than 21 billion tons of garbage per year [28]. Therefore, recycling textiles is inevitable, and all the top brands are now demanding this from the textile industry to recycle their products. Existing textile recycling methods include incineration, landfills, monomer recovery, and reclamation of the fibers from used apparel. All these techniques are not without their limitations, and a permanent solution for textile waste recycling is far from realized [27]. One solution could be to convert the textile synthetic waste into value-added carbon black. The carbon black based upon textile waste costs about half the price of commercial carbon black as the raw material comes from the waste and around 50% of cost of carbon black comes from its raw material [29, 30]. Carbon black has been employed in numerous applications reported in the literature [31–34]. At present, carbon black is synthesized by petroleum sources [35]. Concerns about global warming due to the use of fossil fuels and the large reliance on carbon material generation through petroleum supplies and its rising prices have prompted scientists to seek eco-friendly carbon alternatives, and similar work has been reported in the scientific literature [36–42]. Recently, researchers have focused on using eco-friendly materials derived from recycling [43]. Research is going on at present where carbon materials have been synthesized from lignin-based materials, lignocellulosic materials, and oil is obtained after the pyrolysis of biomass. Renewable source-based precursors have gained a lot of interest due to their abundance in nature and good structural properties [44, 45]. From the literature, it has been observed that carbon material obtained from natural sources such as corncob, when mixed with iron-based materials, exhibits a good photo-Fenton degradation effect, and breaks down organic pollutants in water [46]. Carbon black based on textile waste has been reported in literature for structural and energy applications [5, 47] but carbon black particularly based on the waste fabric from polyester 100% and polyester cotton blend (50:50) waste has not been reported in the literature yet.

The conductive inks market is increasing day by day, and according to statistics, by 2024, it will reach a mammoth USD 4.37 billion. In the wearable and smart electronics fields, the demand for cheap and readily available materials is increasing, and it is expected that this sector will provide the catalyst for the demand for conductive inks [48, 49]. Flexible conductive inks printed circuits on textile fabrics are expected to replace expensive copper wires and silver-based circuits, are easy to embed in the fabric, and are comfortable next to the skin. Similar studies have been reported in the literature [50–52]. Conductive inks, due to their small size, have better durability and efficiency than wires and circuits. In metals, silver is at the top of the list in electronic circuit applications owing to its high conductivity and oxidation stability [53, 54]. Unfortunately, silver is expensive, and the industry is shifting towards cheaper alternatives such as copper, aluminum, graphene, and carbon black-based inks [55, 56]. Conductive inks based on graphene can exhibit properties comparable to those of silver and copper-based conductive inks in RIFD antennas [57–59].

Furthermore, only a handful of companies worldwide produce these highly in-demand conductive inks [60, 61]. The advantages of using carbon black are its abundant supply, ease of processing, low cost, and reinforcing effect [62]. Carbon black has a high specific surface area compared to graphite and can disperse easily into solvents. Carbon nanotubes and graphene are expensive materials and dispersing them in solutions is an arduous job [63]. Carbon black on the other hand can be easily dispersed and used to accomplish electromagnetic wave absorption, which is a significant issue with graphene due to its higher conductivity, which causes impedance mismatch [64]. Moreover, the lab synthesized carbon black, which could be used for other applications such as conductive ink-printed circuits, electromagnetic shielding devices, and high-strength flexible conductive paper fabrication owing to low cost and more availability with good electrical properties comparatively [65–69]. The synthesis of carbon black based on predominately synthetic textile waste and subsequent applications to conductive inks is yet to be reported in the literature [70].

In this study, we successfully report the synthesis of good quality carbon black from waste polyester and polyester-cotton blend (50:50) fabrics as a replacement of fossil fuels.

Carbon black was synthesized from waste fabrics based on polyester-cotton blend (50:50) and 100% polyester in a horizontal tube furnace in an inert environment in a temperature range of 700~1000 °C. Morphology and structure of the obtained carbon black were studied and compared with the commercial carbon black. Conductive inks were formulated by the obtained carbon black and screen printed on 100% cotton fabric. Cyclic voltammetry was carried out to study the conductivity of the printed fabric and compared it with those of commercial carbon black. Textile wearability-based tests such as tensile strength, tear strength, flexural rigidity, air permeability, and crocking fastness (dry and wet) on all the printed fabrics were carried out on all the samples to study the wearability and comfort performance.

2 Materials and methods

- A 100% polyester fabric (PET) and polyester cotton blend (50:50) (PC) waste fabrics were supplied by Interloop Textile Pvt. Ltd.
- A total of 100 g of waste fabric was placed into the horizontal tube furnace KJ-T1600 and then pyrolyzed in a temperature range of 700–1000 °C at a heating rate of 5 °C/min in an inert environment (nitrogen gas) with a holding time of 30 min. Carbon black obtained after pyrolysis was pulverized on an industrial pulverizer Silver Crest SC-350 to a mean value of 10-micron size.
- Commercial carbon black N660 (CCB) was obtained from National Petrocarbon Pvt. Ltd. for comparison purposes.
- Helizarin® LTC New liq. a formaldehyde-free binder, Lutexal® CSFN Liq thickener were obtained from Archroma ltd.
- Printing auxiliaries such as urea, acetic acid, and sodium bicarbonate were bought from Archroma ltd.
- To prepare conductive inks, first stock paste was prepared by taking a calculated amount of the thickener, binder, and distilled water as reported in Table 1. The PH of the stock paste was maintained at 5.5 with the help of acetic acid and sodium bicarbonate.
- After that, conductive ink was synthesized by mixing the calculated amount of carbon black and the stock paste.
- A screen of mesh count 305 mesh/inch was used to apply the print paste on 100% pretreated cotton fabric. Thickener of 3 g/l was used for pretreatment of the fabric to achieve a plain fabric surface.
- After that, drying at 100 °C for 3 min and curing at 180 °C for 5 min were carried out.
- Soaping was carried out manually by using lab-scale surfactant at 40 °C for 5 min followed by cold rinsing with distilled water.

Table 1 Recipe of conductive inks

Recipe of stock paste in 100 g and conductive inks paste in 10 g	
Chemical	Quantity
Thickener	3 g
Helizarin binder	18 g
Distilled water	79 ml
10% Filler percentage	
Filler (carbon black)	1 g
Stock paste	9 g
20% filler percentage	
Filler (carbon black)	2 g
Stock paste	8 g
30% filler percentage	
Filler (carbon black)	3 g
Stock paste	7 g
40% filler percentage	
Filler (carbon black)	4 g
Stock paste	6 g
50% filler percentage	
Filler (carbon black)	5 g
Stock paste	5 g

2.1 Characterizations

2.1.1 Morphology of carbon black

The morphology of the obtained carbon black from the various textile wastes and the commercial carbon black was studied via a scanning electron microscope (AIS 1800C, Korea). All the samples were quoted with a 5 nm layer of gold particles prior to the measurements.

2.1.2 Raman analysis

The carbon structure evolution of the carbon black from the textile wastes were studied via Raman spectroscopy using a green laser of 532 nm wavelength. The instrument used was a Raman microscope (DXR3, US).

2.1.3 Fabric and film thickness

Fabric thickness was measured according to ASTM D1777-96 standard using a HY0141D/E, (China) fabric thickness tester. Film thickness was measured by taking the difference between printed and non-printed samples stated in Eq. 1.

$$T_f = T_p - T_n \quad (1)$$

Where T_f is the film thickness, T_p is printed fabric thickness, and T_n is non-printed fabric thickness.

2.1.4 Electrical conductivity

The electrical characterization of the printed samples was carried out by a 4-probe device connected to a Gamry instruments, USA interface 1010. Samples were cut in the dimensions of 47 mm × 34 mm. Cyclic voltammetry was carried out to obtain IV curves in the range of −0.5~0.5V. Resistance of the printed fabric was measured according to the ohm's law.

$$\boldsymbol{V = IR} \tag{2}$$

Where V is the voltage, I is the current, and R is the resistance of the printed patch.

The thickness of the films was calculated by subtracting fabric thickness as exhibited in Fig. 1. The area of the printed patch was calculated by multiplying length and width. The resistivity of the printed fabric was calculated by the formula [71] stated in Eq. 3.

$$\boldsymbol{\rho = Rs \times Tf} \tag{3}$$

where ρ is the resistivity, Rs is the resistance, and Tf is the thickness of the film. Conductivity was calculated by the inverse of resistivity as stated in Eq. 4.

$$\mathbf{S} = \frac{\mathbf{1}}{\boldsymbol{\rho}} \tag{4}$$

where S is the conductivity and the value of conductivity obtained in $ohm^{-1}m^{-1}$ (Siemens.)

2.1.5 Dry rubbing fastness

The dry rubbing fastness was measured using AATCC 08 standard test method. At first, all samples were conditioned according to the ASTM D1776 method. Then samples were cut into the dimensions of 50 mm × 130 mm. Crock square (bleached white cloth) was mounted on the peg and the printed sample was mounted on the crock meter base. Then, the peg was lowered to touch the printed fabric surface and rubbed 10 times against each other. Afterwards, the crock square was conditioned at the standard temperature of 21± 1 °C and relative humidity of 65±2% and its rating was evaluated by the grey scale.

2.1.6 Wet rubbing fastness

The wet rubbing fastness test was carried out according to the AATCC 08 standard. First, a crock square (white-bleached cloth) was soaked in distilled water to achieve a wet pickup of 65 ± 5%. Then, crock square was mounted on the peg and the printed sample was mounted on the crock meter base. After that, the peg was lowered to touch the printed fabric surface and rubbed 10 times against the printed fabric surface. Afterwards, the crock square was dried and conditioned. Rating was done by using the grey scale.

2.1.7 Air permeability

The air permeability test was carried out by following ASTM D737-96 standard using a HY0461L (China) air permeability tester. Circles of fabric were placed on the sample holder. The test was carried out from five different places of the specimen by passing high-pressure air through a nozzle. The offset area die was selected according to the fabric. A die of size 4.5 inches/114 mm was used. Air permeability values were calculated in mm/sec.

2.1.8 Tear strength

Fabric tear strength test was carried out by using an SDL ATLAS M008HE tear tester according to the ASTMD-1424

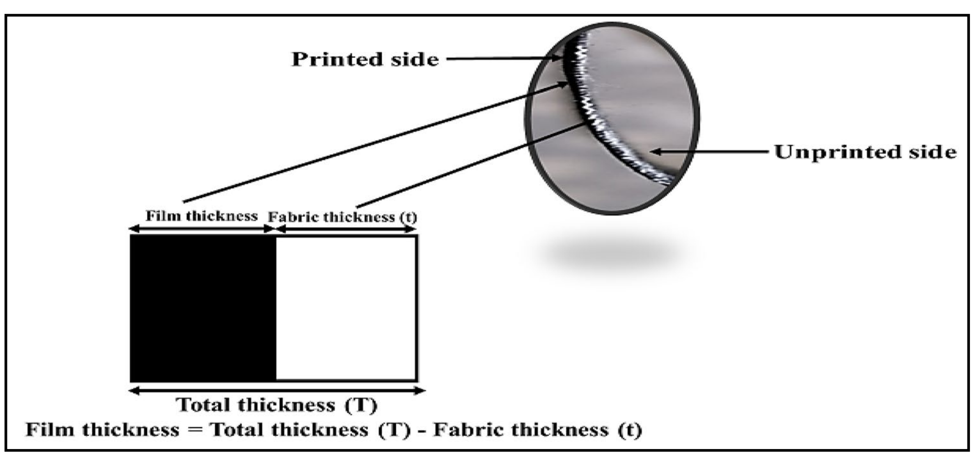

Fig. 1 Top view of the screen-printed film on the substrate

standard. The fabric strips along warp and weft were cut into 76.2 mm × 101.6 mm from 5 different places of the fabric. Every specimen was pre-notched with a 12.7 mm × 12.7 mm notch at the center from the top of the fabric and measured with the load of 1600 CN.

2.1.9 Tensile strength

Fabric tensile test was conducted according to the ASTMD-5035 standard on the M500-50 AT, (U.K) tensile strength tester. The fabric strip along the warp and weft was cut into 25.4 mm × 150 mm from 5 separate places of the fabric and measured at the extension rate of 300 ± 10 mm/min.

2.1.10 Bending rigidity

The bending stiffness of the fabric was measured according to ASTM D1388-18 standard. Samples were cut in 25 mm × 200 mm dimensions, and their bending lengths were calculated on a cantilever stiffness measurement equipment. Bending rigidity (flexural rigidity) of the fabrics was calculated through the formula.

$$G = Wc^3 \tag{5}$$

where G is bending rigidity, w is the GSM of the fabric, and c is half of the fabric bending length.

2.1.11 Fabric washing

The washing test was carried out according to the BS EN ISO 105-C06 standard test method on a M228BC (U.S) Rota wash SDL Atlas machine. A1M multiple washing test number was selected. Samples were cut according to the same size of multi-fiber strip 40 mm*100 mm and one edge was sewn. The solution recipe was made according to the calculated amount of ECE phosphate 4 g/L and sodium perborate 1 g/L. Specimens were added to the Rota wash beaker with 10 steel balls and washed for 40 min at 40 °C.

3 Results and discussion

3.1 Morphology of carbon black

The morphology of the various carbon black is depicted in Fig. 2. It is evident that that the PC-based carbon black exhibits a fiber like structure due to the presence of cotton fibers in its constituents, while PET, that arises from the synthetic fiber background, forms a brittle rhombus like geometry after pyrolysis. On the other hand, the commercial carbon black exhibits a round morphology with agglomerates of the carbon black particles owing to small size. The fiber like structure of PC-based carbon black may help in superior conductivity properties owing to the higher particle to particle connectivity that is of paramount importance in such studies [72].

3.2 Structural properties

The Raman spectra of the various carbon black are depicted in Fig. 3. The obtained carbon black from textile waste exhibits typical spectra of semi-crystalline to amorphous materials as the temperature of pyrolysis is shifted towards the lower side [73]. The Raman spectra of the carbon black exhibited characteristic D and G peaks related to carbon materials [74]. D peak is related to the defective graphite like structures while the G-peak arises owing to the sp^2 carbon bonds in-plane stretching [75]. The D and G peaks were fitted with a Gaussion-Lorentzian shape function (GauLor) to estimate the area under the peaks [76]. I_D/I_G ratio, that represents the degree of structural order in a material [77], was estimated from the area under the D and G peaks as reported in Table 2.

It is evident from the results that as the temperature of the pyrolysis increases, the I_D/I_G ratio decreases indicating towards a greater degree of order owing to the release of volatile substances from the PC and PET precursors and ordering of structure due to higher molecular mobility at higher temperatures [78]. As the temperature of pyrolysis rises, the broad D-peak sharpens up indicating towards a

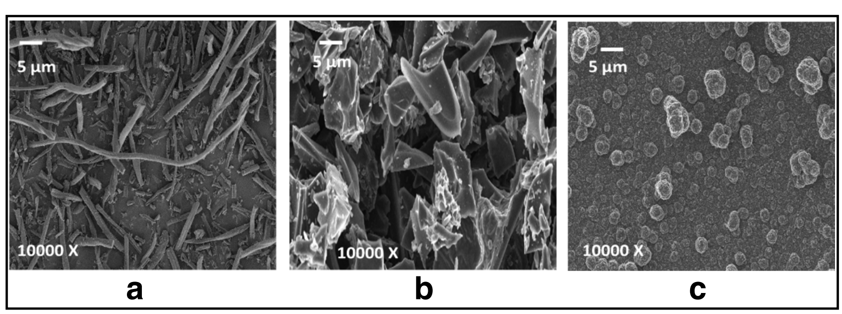

Fig. 2 Morphology of carbon black **a** PC, **b** PET, and **c** CCB

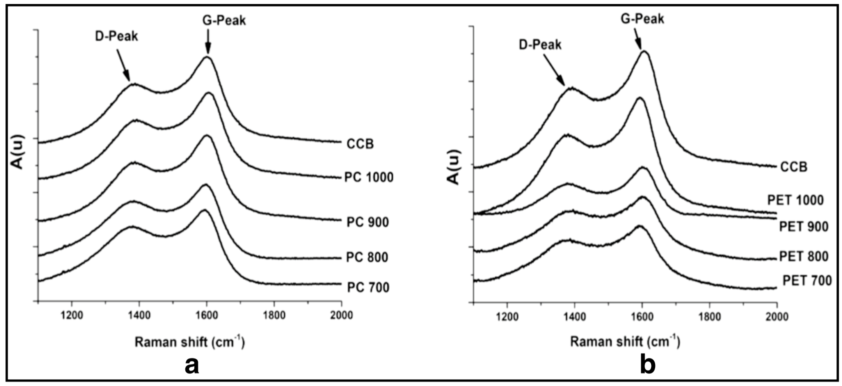

Fig. 3 Raman spectra comparison of **a** PC-based CB and **b** PET-based CB with CCB

Table 2 D-peak, G-peak, and ID/IG ratio comparison of PC- and PET-based CB with CCB

S.no	Sample ID.	D-Peak position	G-Peak position	I_D/I_G	Sample ID.	D-Peak position	G-Peak position	I_D/I_G
1	PC 700	1370	1590	0.92	PET 700	1366	1595	0.94
2	PC 800	1373	1594	0.94	PET 800	1372	1598	0.96
3	PC 900	1378	1595	0.89	PET 900	1375	1601	0.93
4	PC 1000	1382	1603	0.85	PET 1000	1377	1604	0.91
5	CCB	1384	1600	0.89	CCB	1385	1605	0.89

reduction in the structural defects owing to the higher kinetic energy of the molecules provided by the high temperature and better rearrangement of the molecular chains after the exclusion of volatile materials. The lower I_D/I_G ratio of PC carbon black indicates a more ordered structure when compared to the PET-based carbon black and CCB. The higher structural order of the PC carbon black indicates towards a more graphite like structure that can enhance the electrical and thermal conductivity of the subject carbon black [79].

3.3 Electrical conductivity

Electrical characterization of conductive printed fabric, depicted in Fig. 4, was carried out using a 4-probe electrode connected to a Gamry instrument interface 1010.

3.3.1 Before washing

It is evident from the results that the fabric printed with carbon black obtained from PC waste exhibited the maximum value of conductivity followed by the commercial carbon black-based fabric and PET waste-based carbon black printed fabrics. Before washing the printed fabric samples, the value of conductivity of carbon black obtained from PC waste at 700 °C and 10% filler percentage was 1.77*10^2 S/m and at 50% filler percentage, it was around 2.33*10^2 S/m. Commercial carbon black exhibited slightly higher value of conductivity of 2.47*10^2 S/m at same pyrolysis temperature and filler percentage. In case of same filler percentage at higher pyrolysis temperature of 1000 °C, the value of conductivity of carbon black from PC waste was 2.63*10^2 S/m which was 6.19% more than commercial sample and 12.89% more than carbon black obtained from polyester waste probably due to the higher particle to particle connectivity owing to its fiber like morphology. The increase in conductivity of cotton fabric printed with lab-grown carbon black is most likely due to carbon black's ability to conduct electricity. As the percentage of carbon black in the print paste or on the fabric's surface increases, more conductive paths are formed, allowing electricity to flow through the fabric. The printed carbon black particles create a network of conductive pathways on the substrate and thus increase the conductivity of the fabric. When the

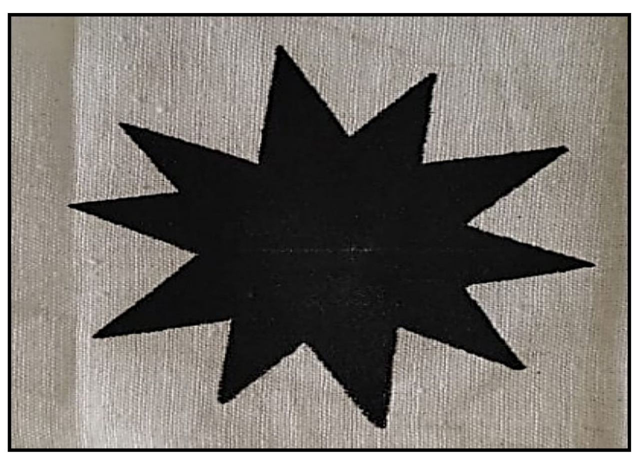

Fig. 4 Conductive ink printed fabric

concentration of carbon black particles increases, so does the number of conductive pathways, resulting in greater overall conductivity [80]. The reason of higher conductivity at higher pyrolysis temperature is due to the production of a more ordered and crystalline structure of carbon black particles, carbon black that is synthesized at higher temperatures typically displays higher conductivity [81, 82]. At higher temperatures, the carbon black particles experience a conversion of the precursor materials into carbon that is both completer and more efficient than at lower temperatures. This leads to the synthesis of carbon black that is more highly graphitized [79, 83]. Graphitized carbon black has a structure that is more organized and crystalline, which results in improved conductivity and a more efficient transfer of electrons [84]. Additionally, synthesis carried out at higher temperatures can also result in smaller particle sizes. This can increase the surface area-to-volume ratio of the carbon black particles, which in turn offers more opportunities for electrons to move between particles and makes the transfer of electrons between conductive pathways easier [85]. Similar studies have been reported by several authors in the literature where the electrical conductivity of carbon materials is governed by the carbonization temperatures [86, 87].

The highest conductivity was exhibited by the PC 1000 printed patch in 50% filler weight which is 6.1% higher than the commercial carbon black and 12.89% higher than the PET-based carbon black at the same filler weight as depicted in Figs. 5 and 6.

3.3.2 After washing

After washing the fabric according to the BS EN ISO 105-C06 standard, the conductivity was measured for all the specimen on four different occasions, i.e., before washing and after 5, 10, and 20 washes to check the performance of printed patch. In the case of 5 domestic washes, the conductivity remained unchanged. After 10 washes, the conductivity was reduced by a cumulative value of 12% as depicted in Figs. 7 and 8.

After washing the printed fabrics, in case of carbon black obtained from PC waste, the range of conductivity was 1.58*10^2 to 2.08*10^2 S/m at temperature range of 700 to 1000 °C and the value of conductivity obtained in case of 10% filler at 700 °C was lower as compared to the value of conductivity obtained at 50% at same temperature and

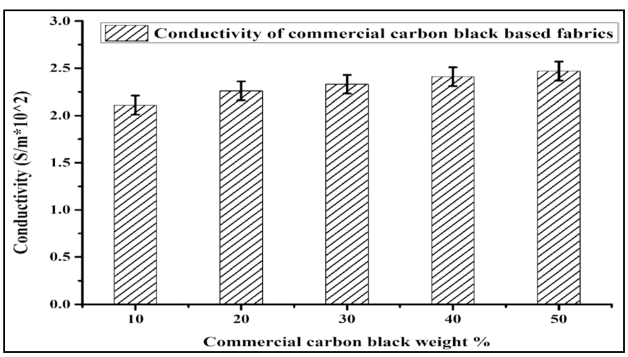

Fig. 5 Conductivity comparison of printed fabric based on commercial carbon black before washing

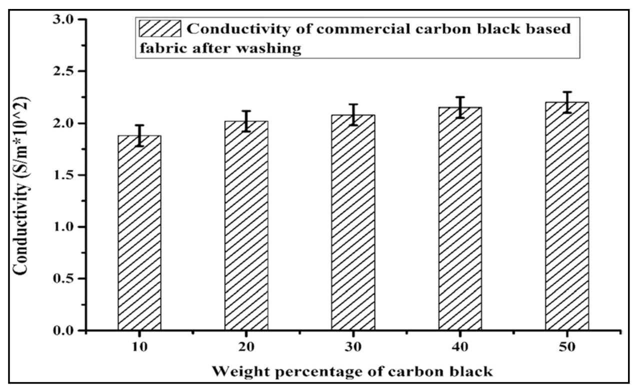

Fig. 7 Conductivity comparison of printed fabric based on commercial carbon black after washing

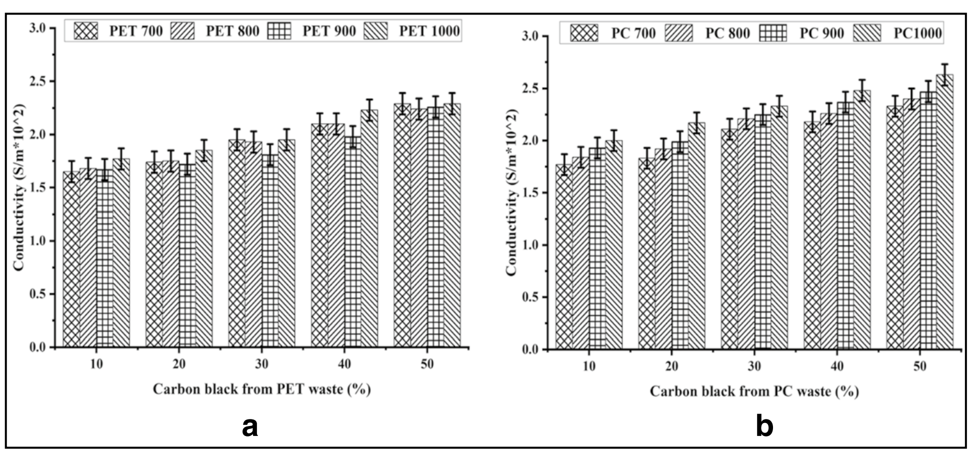

Fig. 6 **a** Conductivity comparison of printed fabric based on carbon black from 100% polyester waste before washing. **b** Conductivity comparison of printed fabric based on carbon black from PC waste before washing

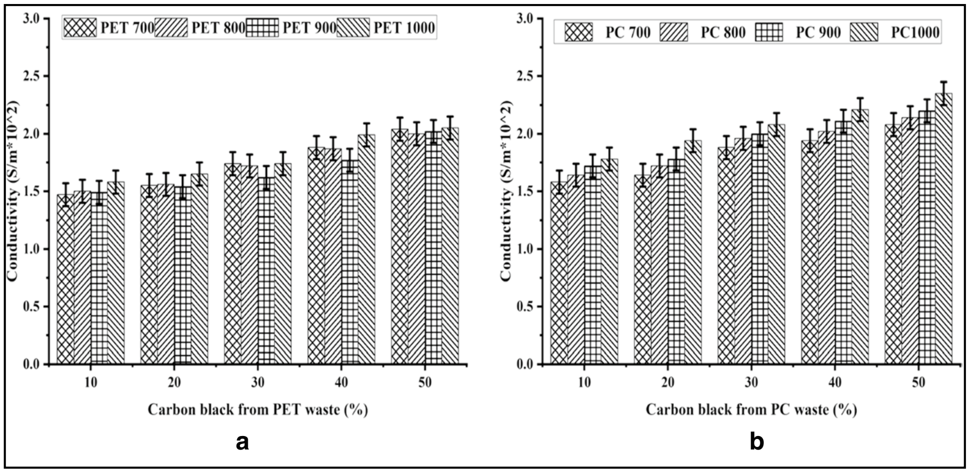

Fig. 8 Conductivity comparison of **a** printed fabric based on carbon black from 100% polyester waste after washing and **b** printed fabric based on carbon black from PC waste after washing

the trend was same for all temperature ranges from 700 to 1000 °C. The value of conductivity of printed carbon black obtained from PC waste at 700 °C pyrolysis temperature exhibited 1.58*10^2 S/m at 10% filler percentage. On the other hand, the value of conductivity of carbon black printed fabric obtained at pyrolysis temperature of 1000 °C exhibited a conductivity of 2.35*10^2 S/m. The value of conductivity obtained in case of commercial carbon black was 6.1% lower than PC and 7.68% higher than carbon black obtained from PET at the same pyrolysis temperature of 700 °C. And after 20 domestic washes, the conductivity dropped by 30% in comparison to the before washing values for all samples. This loss in conductivity is associated to the loss of carbon filler owing to the complex mechanism of washing cycles such as bending, torsion, friction, chemical influence, water stresses, and thermal stresses [88]. Mechanical action is by far the most damaging factor and during washing, two types of mechanical action generate the first type of mechanical action between steel balls and printed fabric and the second type of mechanical action between fabric and walls of the beaker during the rotation [89] that loosen up the filler particles from the inks and causing a disruption in the connection between the particles and hence conductivity reduces.

3.4 Crocking fastness

According to the findings, it is clear that the fabric that was printed with conductive inks containing commercial carbon black displayed inferior fastness properties in comparison to the fabric that was printed with conductive inks containing carbon black manufactured in the laboratory. As the percentage of fillers in the sample increases from 10 to 50%, the rating of the sample's fastness declines from good to poor. This pattern is seen in each and every one of the samples. This fall in fastness rating may be related to the filler particles becoming dislodged from the binder as a result of the application of rubbing force, particularly at higher filler percentages. This phenomenon is more likely to occur at higher filler percentages [90]. It has been reported that binder concentration holds a significant impact on the printed fabric properties such as dry and wet rubbing fastness [91]. Binder forms a film and entraps the filler particles under that film. When the percentage of the filler increases, the amount of the binder decreases and thinner film will be formed making it difficult to hold the filler particles inside the film during the application of the rubbing/ frictional force and thus a reduction in the rating would be observed [92]. The crocking ratings of the various samples are depicted in Tables 3, 4, and 5.

3.5 Tear strength

The tear strength of the fabric plays an important role in fabric performance. The results of the tear strength of the various printed fabrics are depicted in Figs. 9 and 10. It is evident that the tear strength of the printed fabric decreased with the increase of the filler percentage. The value of tear strength is less in the case of commercial carbon black printed fabric, although the trend of tear strength is the same in both cases. The tearing area of the sample is called the del zone which arises due to the slippage and stretching of the yarns parallel to the tearing force (longitudinal yarns) along with transverse yarns due to jamming and stretching. A higher decrease in the tear strength of the commercial carbon black printed fabric can be associated

Table 3 Crocking fastness comparison of printed fabric based on commercial carbon black

Crocking fastness of conducting inks made from commercial carbon black					
Percentage	10%	20%	30%	40%	50%
Dry rubbing fastness	3/4	3	3	2/3	2/3
Wet rubbing fastness	2/3	2/3	2/3	1/2	½

Table 4 Crocking fastness comparison of conducting inks based on carbon black from PC (50:50) waste

Crocking fastness of conducting inks based on carbon black from pc (50:50) waste											
Fastness	PC 700					Fastness	PC 800				
	10%	20%	30%	40%	50%		10%	20%	30%	40%	50%
Dry rubbing	4/5	4	4	3/4	3/4	Dry rubbing	4/5	4/5	4/5	4	4
Wet rubbing	4	3/4	3/4	3	3	Wet rubbing	4	3/4	3	3	3
Fastness	PC 900					Fastness	PC 1000				
	10%	20%	30%	40%	50%		10%	20%	30%	40%	50%
Dry rubbing	5	4/5	4	4	3/4	Dry rubbing	4/5	4	4	3/4	3/4
Wet rubbing	4	3/4	3	3	2/3	Wet rubbing	4	3	3	3	3/4

Table 5 Crocking fastness comparison of conducting inks based on carbon black from 100% polyester waste

Crocking fastness of conductive inks made from polyester waste											
Fastness	PET 700					Fastness	PET 800				
	10%	20%	30%	40%	50%		10%	20%	30%	40%	50%
Dry rubbing	5	4/5	4/5	3/4	3/4	Dry rubbing	5	4/5	4/5	4	4
Wet rubbing	4	4	3/4	3	3	Wet rubbing	4	3/4	3/4	3	3/4
Fastness	PET 900					Fastness	PET 1000				
	10%	20%	30%	40%	50%		10%	20%	30%	40%	50%
Dry rubbing	5	4/5	4	4	3/4	Dry rubbing	5	4/5	4/5	4	3/4
Wet rubbing	4	3/4	3	3/4	3/4	Wet rubbing	4/5	4	3/4	3/4	3

to the restriction of yarn mobility during the application of force as reported in literature by several authors [93]. As the filler percentage increased, the carbon black particles filled the empty spaces between the yarns and create hindrance for yarn mobility upon application of the stress and thus tear strength reduced [94].

3.6 Air permeability

Results of air permeability are depicted in Figs. 11 and 12. It is evident that the commercial-grade carbon black printed fabric exhibits a lower permeability than the value compared to its counterparts. Also, when the percentage of filler (carbon black) increases from 10 to 50%, the rate of airflow decreases but the lab grown carbon black printed fabrics exhibit a better airflow rate compared to the commercial carbon black printed fabric. It has been reported in the literature that the airflow resistivity is inversely proportional to fabric porosity [95]. Woven fabric voids, generated by the interlacement of warp and weft yarn, and fabric thickness affect the rate of airflow of the fabric. So due to high percentage of filler in print paste causes an increase in GSM of fabric [96] as well as block the voids so the air permeability rate might be reduced due to the filling volume of voids of woven fabric [97]. The lower air permeability of the commercial carbon black printed fabric can be associated to its higher surface area that blocked the fabric voids and pores and resulted in a lower air flow.

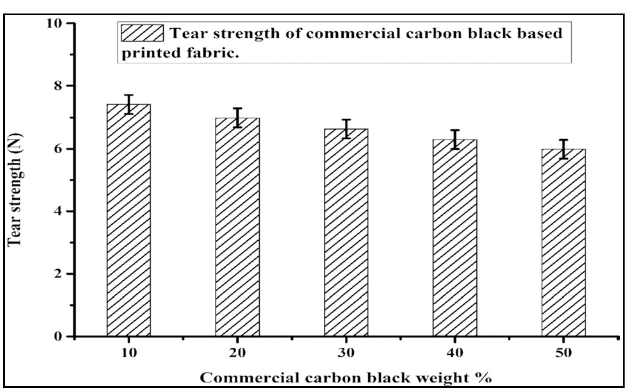

Fig. 9 Tear strength comparison of printed fabric based on commercial carbon black

3.7 Tensile strength and elongation

The tensile strength of the printed fabric is depicted in Figs. 13 and 14. The tensile strength of all the printed fabrics increases when the filler percentage increases from 10 to 50%. On the other hand, the percentage of elongation decreases due to the increase in filler percentage shown in Figs. 15 and 16. The tensile strength of the fabric depends on its binding points. When the percentage of filler increases in the printing paste, upon application to the fabric, the carbon black particles fill the empty spaces between the yarns and thus increase the binding/joining

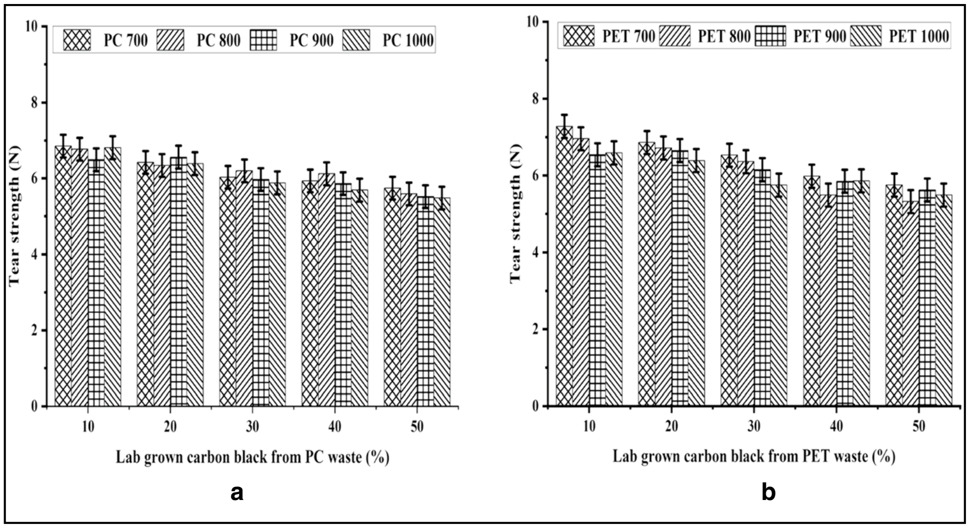

Fig. 10 Tear strength comparison of **a** printed fabric based on carbon black from PC waste and **b** printed fabric based on carbon black from 100% polyester waste

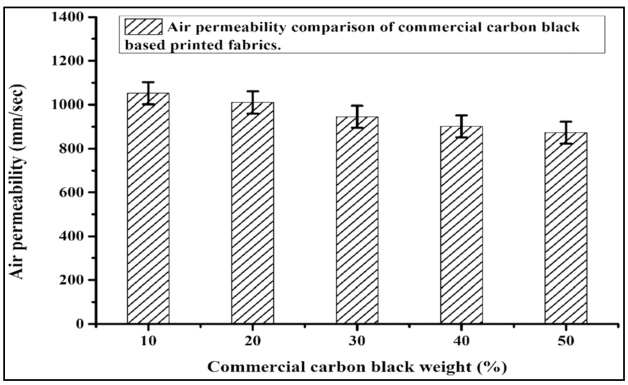

Fig. 11 Air permeability comparison of printed fabric based on commercial carbon black

points. The higher the binding points, the higher the tensile strength of the fabric, and the lower the elongation [98]. It has been reported in the literature that when a fabric undergoes an external loading, it dissipates energy by a combination of various complex mechanisms in which strain energy arises due to the stretching of the yarn; on the other hand, frictional dissipation occurs due to the inter yarn interaction [99]. Inter-yarn friction helps the transmission of stress within the fabric because of contact between yarns [100] and restrains the movement of yarn due to constraints imposed by neighboring yarns [101]. Similar trends can be seen for fabrics printed by the commercial carbon black and the lab grown carbon black.

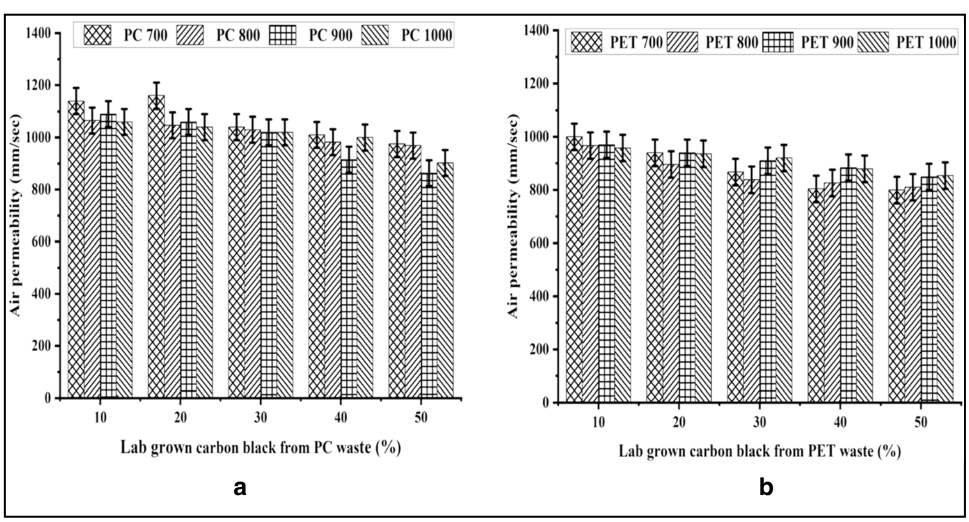

Fig. 12 Air permeability comparison of **a** printed fabric based on carbon black from PC waste and **b** printed fabric based on carbon black from 100% polyester waste

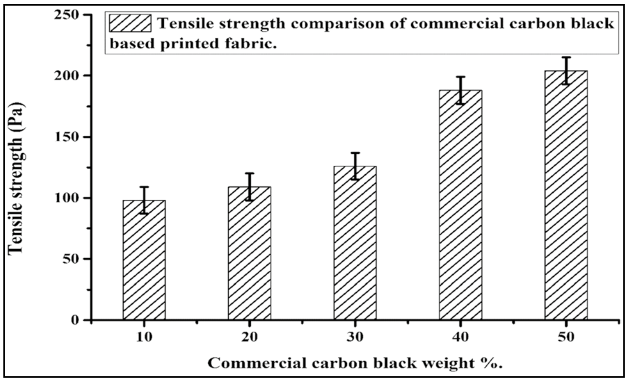

Fig. 13 Tensile strenght comparison of printed fabric based on commercial carbon black

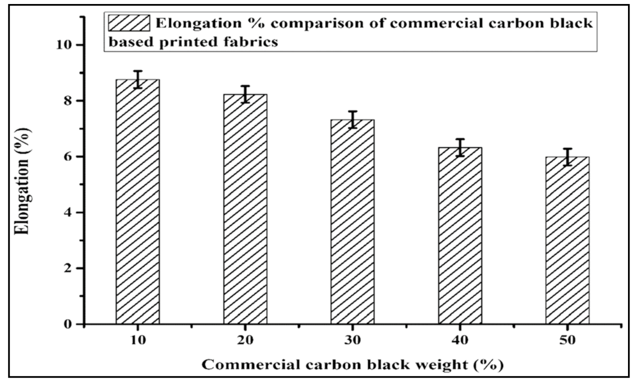

Fig. 15 Elongation percentage comparison of printed fabric based on commercial carbon black. The drop in the elongation of the commercial carbon black printed fabric is probably due to its inherent stiffness. Further investigation in this regard is needed to ascertain this phenomenon, beyond the scope of this work

3.8 Flexural rigidity

From the results, it is evident that the values of flexural rigidity are about the same or closer between commercially available carbon black and lab-synthesized carbon black, as depicted in Figs. 17 and 18. The trend is also similar between the lab grown carbon blacks. As the percentage of the filler increased in the printing paste, the bending length and consequently the bending rigidity of the fabrics increased. This increase could be associated with the increasing value of fabric weight (grams per square meters). GSM has a direct relationship with flexural rigidity because when the percentage of filler is higher in the printing paste, more carbon black will be present on the surface of the fabric to increase the weight of the fabric [102]. The bending length of the fabric also depends on the relative mobility of the fibers in the yarns or yarns in the fabric, so in the case of printed fabrics, the mobility is constrained owing to the carbon black particles hindering the yarns movement consequently leading to an increase in bending length and flexural rigidity [103].

A comparison can be drawn on the properties and performance of the commercial carbon black and the lab grown carbon black as reported in Table 6. The lab grown CB is relatively cheaper than the commercial counterpart as the starting material is an industrial waste and available for free in millions of tons every year. The structure of the lab grown carbon black can be modified by altering the carbonization temperature while the commercial carbon black properties are not tunable via carbonization. The lab grown CB possesses better electrical properties owing to a better internal structure governed by the carbonization temperature.

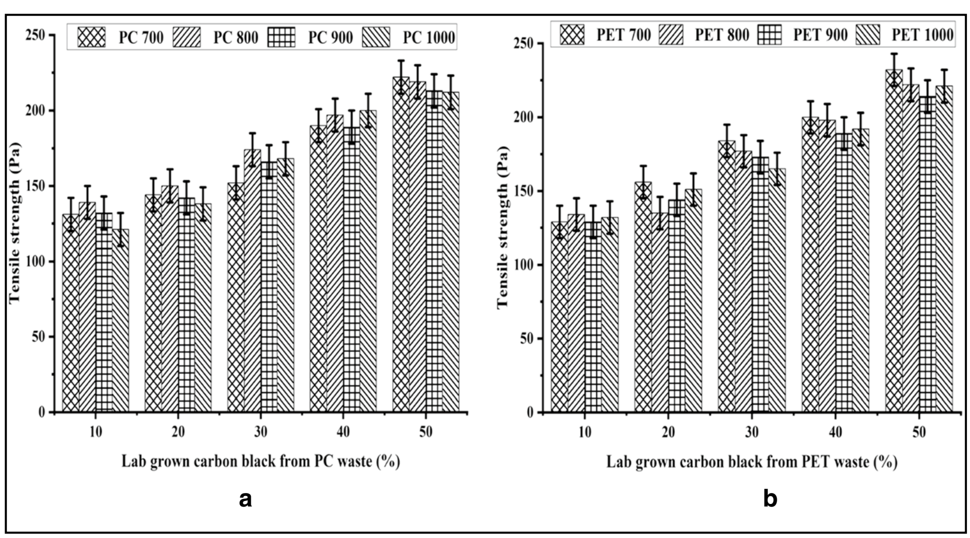

Fig. 14 Tensile strength comparison of **a** printed fabric based on carbon black from PC waste and **b** printed fabric based on carbon black from 100% polyester waste

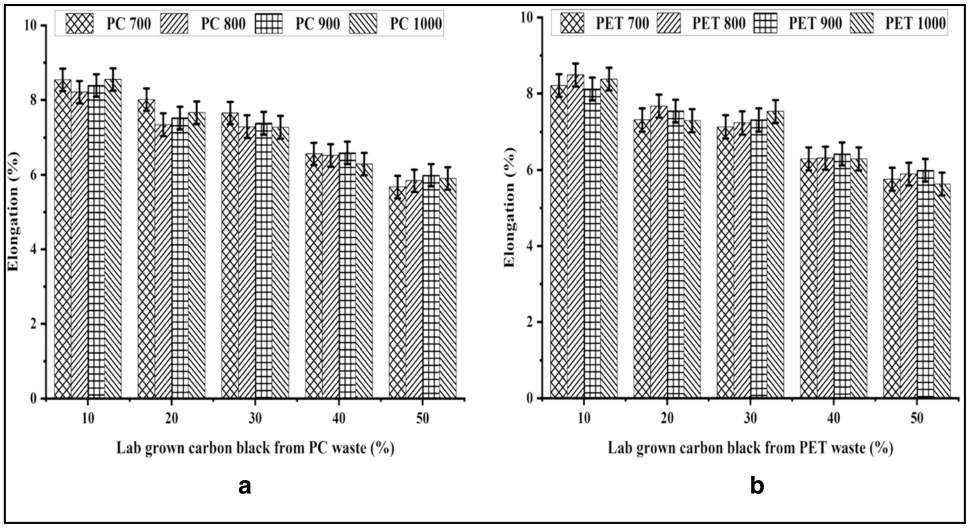

Fig. 16 Elongation comparison of **a** printed fabric based on carbon black from PC waste and **b** printed fabric based on carbon black from 100% polyester waste

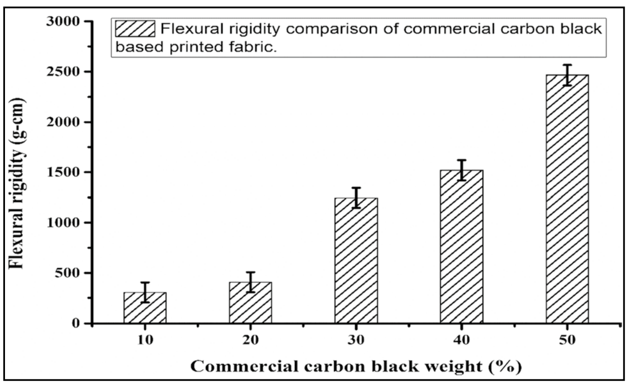

Fig. 17 Flexural rigidity comparison of printed fabric based on commercial carbon black

Based on the above results, we can safely recommend the carbon black synthesized from textile waste as an alternative to the commercial grade carbon black.

4 Conclusion

From the above results, it can be safely concluded that carbon black can be successfully synthesized from textile waste with good conductive properties at a temperature range of 700~1000 °C. Carbon black based on textile waste (polyester-cotton (50:50) blend) exhibited good structural properties in comparison to the commercial carbon black as evident from the Raman spectra. Conductive inks were successfully

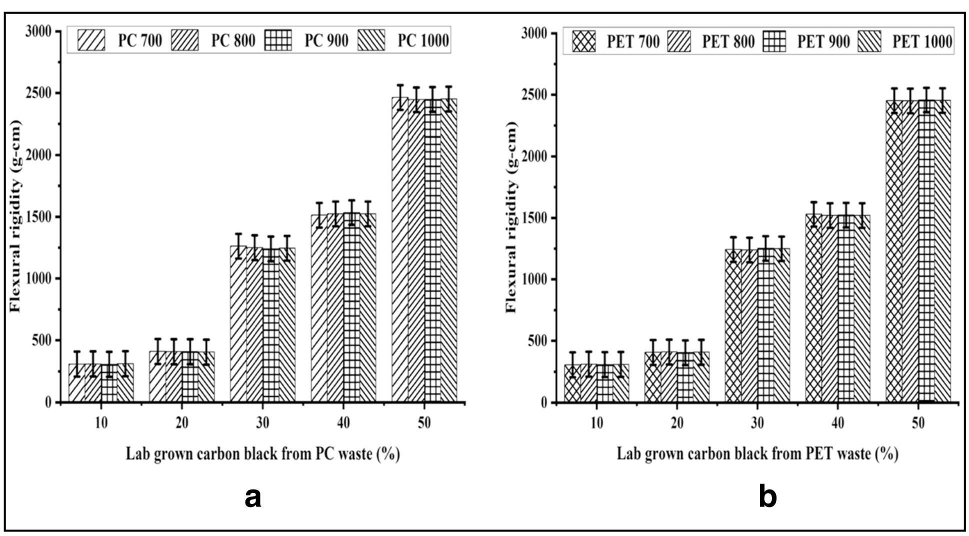

Fig. 18 Flexural rigidity comparsion of **a** printed fabric based on carbon black from PC waste and **b** printed fabric based on carbon black from 100% polyester waste

Table 6 Comparison of properties of commercial and lab grown carbon black

Sr #	Item	Cost per kg	Conductivity of the printed patch at 50% loading of CB	Structure	Process of synthesis	Washing stability of the textile after printing	Mechanical properties of the printed substrate
1	Commercial carbon black	>1 $	2.47*10^1 S/m	Semi crystalline	Thermal cracking	Up to 5 washes	Good
2	Lab grown carbon black	≤ 0.7 $	2.63*10^2 S/m	Semi crystalline to amorphous	Pyrolysis and carbonization	More than 5 washes	Excellent

formulated from the textile waste-based carbon black and electrical properties were compared with the commercial carbon black. Carbon black based on the polyester-cotton blend (50:50) exhibited better conductivity owing to a better graphitic structure compared to the commercial carbon black. The printed patches exhibited good washing stability and conductivity remained almost unchanged after 5 washes. Textile-based analysis such as tensile, tear, air permeability, flexural rigidity, and crock fastness (dry and wet) properties basically depict the serviceability of any fabric. The different analysis depicted that carbon black printed fabrics can be used in apparel with good service life on an industrial scale. The negative connotation attached to lab grown conductive carbon black is that its yield is temperature dependent and at lower temperature, it gives higher yield with low value of conductivity. Further research will be focused on the production of the lab grown carbon black using a wide range of textile wastes and their subsequent application to wearable electronics with an in-depth analysis of the electrical properties of the fabricated materials.

Acknowledgements The authors would like to thank Interloop Textiles Pvt. Ltd. for the provision of Polyester Cotton (50:50) and 100% Polyester waste fabrics. Archroma Ltd for the supply of binder, thickener, and other printing auxiliaries.

Author contribution Study conception, design, and analysis were performed by Dr. Aamer Abbas Khan. Material preparation, data collection, and manuscript writing were done by M. Awais Rasool. Final review of the manuscript was done by Dr. Muhammad Mohsin.

Funding This research work was funded by Punjab higher education commission (Grant no. PHEC/ARA /PIRCA/20324/14).

Data availability Data and materials will be made available on request.

Declarations

Ethical approval Not applicable

Conflict of interest The authors declare no competing interests.

References

1. Shirvanimoghaddam K, Motamed B, Ramakrishna S, Naebe M (2020) Death by waste: fashion and textile circular economy case. Sci Total Environ 718:137317. https://doi.org/10.1016/J.SCITOTENV.2020.137317
2. Li X, Wang L, Ding X (2021) Textile supply chain waste management in China. J Clean Prod 289:125147. https://doi.org/10.1016/J.JCLEPRO.2020.125147
3. Nørup N, Pihl K, Damgaard A, Scheutz C (2018) Development and testing of a sorting and quality assessment method for textile waste. Waste Manag 79:8–21. https://doi.org/10.1016/J.WASMAN.2018.07.008
4. (2015) Handbook of Sustainable Apparel Production. Handbook of Sustainable Apparel Production. https://doi.org/10.1201/B18428
5. Yousef S, Kalpokaitė-Dičkuvienė R, Baltušnikas A et al (2021) A new strategy for functionalization of char derived from pyrolysis of textile waste and its application as hybrid fillers (CNTs/char and graphene/char) in cement industry. J Clean Prod 314:128058. https://doi.org/10.1016/J.JCLEPRO.2021.128058
6. Istrate IR, Galvez-Martos JL, Dufour J (2021) The impact of incineration phase-out on municipal solid waste landfilling and life cycle environmental performance: case study of Madrid Spain. Sci Total Environ 755:142537. https://doi.org/10.1016/J.SCITOTENV.2020.142537
7. Yasin S, Sun D (2019) Propelling textile waste to ascend the ladder of sustainability: EOL study on probing environmental parity in technical textiles. J Clean Prod 233:1451–1464. https://doi.org/10.1016/j.jclepro.2019.06.009
8. Cesar da Silva P, de Oliveira C, Neto G, Ferreira Correia JM, Pujol Tucci HN (2021) Evaluation of economic, environmental and operational performance of the adoption of cleaner production: survey in large textile industries. J Clean Prod 278. https://doi.org/10.1016/j.jclepro.2020.123855
9. Luo Y, Song K, Ding X, Wu X (2021) Environmental sustainability of textiles and apparel: a review of evaluation methods. Environ Impact Assess Rev 86:106497. https://doi.org/10.1016/J.EIAR.2020.106497
10. Ohara T, Yuasa K, Kimura K et al (2023) A novel mechanical plant compression system for biomass fuel and acquisition of squeezed liquid with water-soluble lignin as anti-virus materials. J Mater Cycles Waste Manag 25:249–257. https://doi.org/10.1007/S10163-022-01531-5/FIGURES/3
11. Sonu RGM, Pathania D et al (2023) Agro-waste to sustainable energy: a green strategy of converting agricultural waste to nano-enabled energy applications. Sci Total Environ 875:162667. https://doi.org/10.1016/J.SCITOTENV.2023.162667
12. Chaudhary V, Gautam A, Silotia P et al (2022) Internet-of-nano-things (IoNT) driven intelligent face masks to combat airborne health hazard. Mater Today 60:201–226. https://doi.org/10.1016/J.MATTOD.2022.08.019
13. Zhu X, Zhang J, Zhou J et al (2022) Adsorption characteristics and conformational transition of polyethylene glycol–maleated rosin polyesters on the water–air surface. Adv Compos Hybrid Mater 5:1233–1240. https://doi.org/10.1007/S42114-021-00354-6/TABLES/2

14. Li Z, Li Y, Lei H et al (2022) The effect of synergistic/inhibitory mechanism of terephthalic acid and glycerol on the puncture, tearing, and degradation properties of PBSeT copolyesters. Adv Compos Hybrid Mater 5:1335–1349. https://doi.org/10.1007/S42114-021-00405-Y/FIGURES/9
15. Shen L, Worrell E, Patel MK (2010) Environmental impact assessment of man-made cellulose fibres. Resour Conserv Recycl 55:260–274. https://doi.org/10.1016/J.RESCONREC.2010.10.001
16. More AP (2021) Flax fiber–based polymer composites: a review. Adv Compos Hybr Mater 5:1–20. https://doi.org/10.1007/S42114-021-00246-9
17. Khanzada H, Khan MQ, Kayani S (2020) Cotton based clothing. Cotton Sci Proc Technol : Gene, Ginn Garment Green Recyc:377–391. https://doi.org/10.1007/978-981-15-9169-3_15
18. Imoisili PE, Adeleke O, Makhatha ME, Jen T-C (2023) Response surface methodology (RSM)- artificial neural networks (ANN) aided prediction of the impact strength of natural fibre/carbon nanotubes hybrid reinforced polymer nanocomposite. https://www.espublisher.com/. https://doi.org/10.30919/ES8D852
19. Devarshi S, Pndhare A, Lokh PE, et al (2023) Natural fibre reinforced thermoplastic composite synthesis methods and potential applications. https://www.espublisher.com/. https://doi.org/10.30919/ESMM5F827
20. Fidan F, Aydoğan EK, Uzal N (2021) An integrated life cycle assessment approach for denim fabric production using recycled cotton fibers and combined heat and power plant. J Clean Prod 287:125439. https://doi.org/10.1016/J.JCLEPRO.2020.125439
21. Pai A, Kini AK, Kini CR, Shenoy SB (2022) Effect of natural fibre-epoxy plies on the mechanical and shock wave impact response of fibre metal laminates. https://www.espublisher.com/ 19:292–300. https://doi.org/10.30919/ES8D730
22. He Y, Zhou M, Mahmoud MHH et al (2022) Multifunctional wearable strain/pressure sensor based on conductive carbon nanotubes/silk nonwoven fabric with high durability and low detection limit. Adv Compos Hybrid Mater 5:1939–1950. https://doi.org/10.1007/S42114-022-00525-Z/FIGURES/7
23. Ma Z, Zhang Z, Zhao F, Wang Y (2022) A multifunctional coating for cotton fabrics integrating superior performance of flame-retardant and self-cleaning. Adv Compos Hybrid Mater 5:2817–2833. https://doi.org/10.1007/S42114-022-00464-9/FIGURES/9
24. Sun J, Shi L, Song T, Sun C (2021) Flame resistance of cotton fabric finishing with N-hydroxymethylacrylamide spirophosphate. Adv Compos Hybrid Mater 4:1155–1165. https://doi.org/10.1007/S42114-021-00348-4/FIGURES/7
25. Wu Y, Huang K, Weng X et al (2022) PVB coating efficiently improves the high stability of EMI shielding fabric with Cu/Ni. Adv Compos Hybrid Mater 5:71–82. https://doi.org/10.1007/S42114-021-00401-2/FIGURES/8
26. Fu B, Shu Z, Liu X (2018) Blockchain enhanced emission trading framework in fashion apparel manufacturing industry. Sustainability 10:1105. https://doi.org/10.3390/SU10041105
27. Sandin G, Peters GM (2018) Environmental impact of textile reuse and recycling – a review. J Clean Prod 184:353–365. https://doi.org/10.1016/J.JCLEPRO.2018.02.266
28. Memon JA, Qayyum M, Aziz A (2020) The rise and fall of Pakistan's textile industry: an analytical view. Eur J Business Manag 12. https://doi.org/10.7176/EJBM/12-12-12
29. León M, Silva J, Carrasco S, Barrientos N (2020) Design, cost estimation and sensitivity analysis for a production process of activated carbon from waste nutshells by physical activation. Processes 8:945. https://doi.org/10.3390/PR8080945
30. Orozco F, Salvatore A, Sakulmankongsuk A et al (2022) Electroactive performance and cost evaluation of carbon nanotubes and carbon black as conductive fillers in self-healing shape memory polymers and other composites. Polymer (Guildf) 260:125365. https://doi.org/10.1016/J.POLYMER.2022.125365
31. Xiao R, Yu G, Bin XB et al (2021) Fiber surface/interfacial engineering on wearable electronics. Small 17:2102903. https://doi.org/10.1002/SMLL.202102903
32. Chen J, Zhang G, Zhao Y et al (2022) Promotion of skin regeneration through co-axial electrospun fibers loaded with basic fibroblast growth factor. Adv Compos Hybrid Mater 5:1111–1125. https://doi.org/10.1007/S42114-022-00439-W/FIGURES/8
33. Afroze JD, Tong L, Abden MJ, Chen Y (2023) Multifunctional hierarchical graphene-carbon fiber hybrid aerogels for strain sensing and energy storage. Adv Compos Hybrid Mater 6:1–13. https://doi.org/10.1007/S42114-022-00594-0/FIGURES/6
34. Deng W, Sun Y, Yao X et al (2022) Masks for COVID-19. Adv Sci 9:2102189. https://doi.org/10.1002/ADVS.202102189
35. Khodabakhshi S, Fulvio PF, Andreoli E (2020) Carbon black reborn: structure and chemistry for renewable energy harnessing. Carbon N Y 162:604–649. https://doi.org/10.1016/J.CARBON.2020.02.058
36. Gao T, Ma Y, Ji L et al (2022) Nickel-coated wood-derived porous carbon (Ni/WPC) for efficient electromagnetic interference shielding. Adv Compos Hybrid Mater 5:2328–2338. https://doi.org/10.1007/S42114-022-00420-7/FIGURES/7
37. Chen W, Lin H, Wu Y et al (2022) Fluorescent probe of nitrogen-doped carbon dots derived from biomass for the sensing of MnO4− in polluted water based on inner filter effect. Adv Compos Hybrid Mater 5:2378–2386. https://doi.org/10.1007/S42114-022-00443-0/TABLES/2
38. Guo Z, Li A, Sun Z et al (2022) Negative permittivity behavior in microwave frequency from cellulose-derived carbon nanofibers. Adv Compos Hybrid Mater 5:50–57. https://doi.org/10.1007/S42114-021-00314-0/FIGURES/6
39. Qi G, Liu Y, Chen L et al (2021) Lightweight Fe3C@Fe/C nanocomposites derived from wasted cornstalks with high-efficiency microwave absorption and ultrathin thickness. Adv Compos Hybrid Mater 4:1226–1238. https://doi.org/10.1007/S42114-021-00368-0/FIGURES/8
40. Sun Z, Qu K, Li J et al (2021) Self-template biomass-derived nitrogen and oxygen co-doped porous carbon for symmetrical supercapacitor and dye adsorption. Adv Compos Hybrid Mater 4:1413–1424. https://doi.org/10.1007/S42114-021-00352-8/FIGURES/6
41. Vijeata A, Chaudhary GR, Umar A, Chaudhary S (2021) Distinctive solvatochromic response of fluorescent carbon dots derived from different components of aegle marmelos plant. Engineered Science 15:197–209. https://doi.org/10.30919/ES8E512
42. Kumari M, Chaudhary GR, Chaudhary S, Umar A (2022) Rapid analysis of trace sulphite ion using fluorescent carbon dots produced from single use plastic cups. Eng Sci 17:101–112. https://doi.org/10.30919/ES8D556
43. Savi P, Josè SP, Khan AA, et al (2018) Biochar and carbon nanotubes as fillers in polymers: a comparison. 2017 IEEE MTT-S International Microwave Workshop Series on Advanced Materials and Processes for RF and THz Applications, IMWS-AMP 2017 2018-January:1–3. https://doi.org/10.1109/IMWS-AMP.2017.8247334
44. Jafari H (2019) Sustainable development by reusing of recyclables in a textile industry including two collectors and three firms: a game-theoretic approach for pricing decisions. J Clean Prod 229:598–610. https://doi.org/10.1016/j.jclepro.2019.04.222
45. Ozturk E, Koseoglu H, Karaboyaci M et al (2016) Sustainable textile production: cleaner production assessment/eco-efficiency analysis study in a textile mill. Elsevier Ltd
46. Sun Z, Zhang Y, Guo S et al (2022) Confining FeNi nanoparticles in biomass-derived carbon for effectively photo-Fenton catalytic

reaction for polluted water treatment. Adv Compos Hybrid Mater 5:1566–1581. https://doi.org/10.1007/S42114-022-00477-4/FIGURES/10
47. Yousef S, Eimontas J, Striūgas N et al (2019) A sustainable bioenergy conversion strategy for textile waste with self-catalysts using mini-pyrolysis plant. Energy Convers Manag 196:688–704. https://doi.org/10.1016/J.ENCONMAN.2019.06.050
48. Zenou M, Grainger L (2018) Additive manufacturing of metallic materials. Elsevier Inc
49. Francis MP, Kemper N, Maghdouri-White Y, Thayer N (2018) Additive manufacturing for biofabricated medical device applications. Elsevier Inc
50. Zhu C, Chalmers E, Chen L et al (2019) A nature-inspired, flexible substrate strategy for future wearable electronics. Small 15:1902440. https://doi.org/10.1002/SMLL.201902440
51. Zhu C, Li R, Chen X et al (2020) Ultraelastic yarns from curcumin-assisted ELD toward wearable human–machine interface textiles. Adv Sci 7:2002009. https://doi.org/10.1002/ADVS.202002009
52. Guo Y, Liu H, Wang D et al (2022) Engineering hierarchical heterostructure material based on metal-organic frameworks and cotton fiber for high-efficient microwave absorber. Nano Res 15:6841–6850. https://doi.org/10.1007/S12274-022-4533-X
53. Mo L, Guo Z, Wang Z et al (2019) Nano-silver ink of high conductivity and low sintering temperature for paper electronics. Nanoscale Res Lett 14:1–11. https://doi.org/10.1186/s11671-019-3011-1
54. Venkata Krishna Rao R, Venkata Abhinav K, Karthik PS, Singh SP (2015) Conductive silver inks and their applications in printed and flexible electronics. RSC Adv 5:77760–77790. https://doi.org/10.1039/c5ra12013f
55. Mendez-Rossal HR, Wallner GM (2019) Printability and properties of conductive inks on primer-coated surfaces. Int J Polym Sci 2019. https://doi.org/10.1155/2019/3874181
56. Pan K, Fan Y, Leng T et al (2018) Sustainable production of highly conductive multilayer graphene ink for wireless connectivity and IoT applications. Nat Commun 9. https://doi.org/10.1038/s41467-018-07632-w
57. Liu L, Shen Z, Zhang X, Ma H (2021) Highly conductive graphene/carbon black screen-printing inks for flexible electronics. J Colloid Interface Sci 582:12–21. https://doi.org/10.1016/j.jcis.2020.07.106
58. Saidina DS, Eawwiboonthanakit N, Mariatti M et al (2019) Recent development of graphene-based ink and other conductive material-based inks for flexible electronics. J Electron Mater 48:3428–3450. https://doi.org/10.1007/s11664-019-07183-w
59. Li W, Sun Q, Li L et al (2020) The rise of conductive copper inks: challenges and perspectives. Appl Mater Today 18:100451. https://doi.org/10.1016/j.apmt.2019.100451
60. Karim N, Afroj S, Tan S et al (2019) All inkjet-printed graphene-silver composite ink on textiles for highly conductive wearable electronics applications. Sci Rep 9:1–10. https://doi.org/10.1038/s41598-019-44420-y
61. Mazhuga PM, Vecherskaya TP (1973) Cytophotometry of DNA content in the nuclei of osteoblasts (Russian). Tsitologiya i Genetika 7:429–431
62. Leblanc JL (2002) Rubber–filler interactions and rheological properties in filled compounds. Prog Polym Sci 27:627–687. https://doi.org/10.1016/S0079-6700(01)00040-5
63. Pantea D, Darmstadt H, Kaliaguine S, Roy C (2003) Electrical conductivity of conductive carbon blacks: influence of surface chemistry and topology. Appl Surf Sci 217:181–193. https://doi.org/10.1016/S0169-4332(03)00550-6
64. Wu X, Liu K, Ding J et al (2022) Construction of Ni-based alloys decorated sucrose-derived carbon hybrid towards: effective microwave absorption application. Adv Compos Hybrid Mater 5:2260–2270. https://doi.org/10.1007/S42114-021-00383-1/TABLES/2
65. Cao S, Ge W, Yang Y et al (2022) High strength, flexible, and conductive graphene/polypropylene fiber paper fabricated via papermaking process. Adv Compos Hybrid Mater 5:104–112. https://doi.org/10.1007/S42114-021-00374-2/FIGURES/4
66. Luo X, Yang G, Schubert DW (2022) Electrically conductive polymer composite containing hybrid graphene nanoplatelets and carbon nanotubes: synergistic effect and tunable conductivity anisotropy. Adv Compos Hybrid Mater 5:250–262. https://doi.org/10.1007/S42114-021-00332-Y/FIGURES/12
67. Liu K, Liu W, Li W et al (2022) Strong and highly conductive cellulose nanofibril/silver nanowires nanopaper for high performance electromagnetic interference shielding. Adv Compos Hybrid Mater 5:1078–1089. https://doi.org/10.1007/S42114-022-00425-2/FIGURES/4
68. Cao X, Jia Z, Hu D, Wu G (2022) Synergistic construction of three-dimensional conductive network and double heterointerface polarization via magnetic FeNi for broadband microwave absorption. Adv Compos Hybrid Mater 5:1030–1043. https://doi.org/10.1007/S42114-021-00415-W/FIGURES/9
69. Cao G, Cai S, Zhang H, Tian Y (2022) High-performance conductive adhesives based on water-soluble resins for printed circuits, flexible conductive films, and electromagnetic interference shielding devices. Adv Compos Hybrid Mater 5:1730–1742. https://doi.org/10.1007/S42114-021-00402-1/FIGURES/6
70. Hemati S, Udayakumar S, Wesley C et al (2023) Thermal transformation of secondary resources of carbon-rich wastes into valuable industrial applications. J Compos Sci 7:8. https://doi.org/10.3390/JCS7010008
71. Naftaly M, Das S, Gallop J et al (2021) Sheet resistance measurements of conductive thin films: a comparison of techniques. Electronics 10:960. https://doi.org/10.3390/ELECTRONICS10080960
72. Phillips C, Al-Ahmadi A, Potts S-J et al The effect of graphite and carbon black ratios on conductive ink performance. J Mater Sci 52. https://doi.org/10.1007/s10853-017-1114-6
73. Ferrari AC, Robertson J (2001) Resonant Raman spectroscopy of disordered, amorphous, and diamondlike carbon. Phys Rev B Condens Matter Mater Phys 64. https://doi.org/10.1103/PHYSREVB.64.075414
74. Merlen A, Buijnsters JG, Pardanaud C (2017) A guide to and review of the use of multiwavelength Raman spectroscopy for characterizing defective aromatic carbon solids: from graphene to amorphous carbons. Coatings 7. https://doi.org/10.3390/COATINGS7100153
75. Ippolito JA, Spokas KA, Novak JM et al (2014) Biochar for environmental management 2 - biochar elemental composition and factors influencing nutrient retention. In: Biochar for environmental management, vol 139. Routledge
76. Tagliaferro A, Rovere M, Padovano E et al (2020) Introducing the novel mixed gaussian-lorentzian lineshape in the analysis of the raman signal of biochar. Nanomaterials 10(9):1748. https://doi.org/10.3390/nano10091748
77. Petrova E, Tinchev S, Nikolova P Interference effects on the I D /I G ratio of the Raman spectra of diamond-like carbon thin films
78. Hansson J, Nylander A, Flygare M et al (2020) Effects of high temperature treatment of carbon nanotube arrays on graphite: increased crystallinity, anchoring and inter-tube bonding. Nanotechnology 31:11. https://doi.org/10.1088/1361-6528/ab9677
79. Khan A, Jagdale P, Castellino M et al (2018) Innovative functionalized carbon fibers from waste: how to enhance polymer composites properties. Compos B Eng 139:31–39. https://doi.org/10.1016/J.COMPOSITESB.2017.11.064

80. Phillips C, Al-Ahmadi A, Potts SJ et al (2017) The effect of graphite and carbon black ratios on conductive ink performance. J Mater Sci 52:9520–9530. https://doi.org/10.1007/S10853-017-1114-6
81. Wang L, Wang X, Zou B et al (2011) Preparation of carbon black from rice husk by hydrolysis, carbonization and pyrolysis. Bioresour Technol 102:8220–8224. https://doi.org/10.1016/J.BIORTECH.2011.05.079
82. Giorcelli M, Savi P, Khan A, Tagliaferro A (2019) Analysis of biochar with different pyrolysis temperatures used as filler in epoxy resin composites. Biomass Bioenergy 122:466–471. https://doi.org/10.1016/J.BIOMBIOE.2019.01.007
83. Potts S-J, Korochkina T, Holder A et al The influence of carbon morphologies and concentrations on the rheology and electrical performance of screen-printed carbon pastes. J Mater Sci 57. https://doi.org/10.1007/s10853-021-06724-1
84. McENANEY B (1999) Structure and bonding in carbon materials. Carb Mater Adv Technol:1–33. https://doi.org/10.1016/B978-008042683-9/50003-0
85. Efig AP-42, CH 6.1: Carbon Black
86. Kwon JH, Park SB, Ayrilmis N et al (2013) Effect of carbonization temperature on electrical resistivity and physical properties of wood and wood-based composites. Compos B Eng 46:102–107. https://doi.org/10.1016/J.COMPOSITESB.2012.10.012
87. Barroso-Bogeat A, Alexandre-Franco M, Fernández-González C et al (2015) Temperature dependence of the electrical conductivity of activated carbons prepared from vine shoots by physical and chemical activation methods. Micro Mesop Mater 209:90–98. https://doi.org/10.1016/J.MICROMESO.2014.07.023
88. Zaman SU, Tao X, Cochrane C, Koncar V (2018) Market readiness of smart textile structures - reliability and washability. IOP Conf Ser Mater Sci Eng 459. https://doi.org/10.1088/1757-899X/459/1/012071
89. Lee A, Seo MH, Yang S et al (2008) The effects of mechanical actions on washing efficiency. Fibers Poly 9:101
90. Forhad Hossain M, Kamruzzaman M, Raza MIAHM et al (2016) Effects of binder and thickeners of pigment printing paste on fastness properties of printed fabric. Int J Sci Eng Res 7:710–716
91. Hussain T, Ahmad M, Masood R (2013) Modelling the properties of pigment-dyed polyester/cotton sheeting fabrics by response surface methodology. Colorat Technol 129:274–278. https://doi.org/10.1111/cote.12040
92. Ibrahim W, Sarwar Z, Khan A et al (2019) A novel study of comparison properties of pigment and reactive dye-printed cotton fabric. J Nat Fibers 16:825–835. https://doi.org/10.1080/15440478.2018.1440364
93. Triki E, Dolez P, Vu-Khanh T (2011) Tear resistance of woven textiles - criterion and mechanisms. Compos B Eng 42:1851–1859. https://doi.org/10.1016/j.compositesb.2011.06.015
94. Eryuruk SH, Kalaoğlu F (2015) The effect of weave construction on tear strength of woven fabrics. Autex Res J 15:207–214. https://doi.org/10.1515/aut-2015-0004
95. Soltani P, Zarrebini M (2013) Acoustic performance of woven fabrics in relation to structural parameters and air permeability. J Text Inst 104:1011–1016. https://doi.org/10.1080/00405000.2013.771427
96. Sundaramoorthy S, Nallampalayam PK, Jayaraman S (2011) Air permeability of multilayer woven fabric systems. J Text Inst 102:189–202. https://doi.org/10.1080/00405001003608147
97. Rainard LW (1946) Air permeability of fabrics. Text Res J 16:473–480. https://doi.org/10.1177/004051754601601001
98. Asaduzzaman M, Hasan AKMM, Patwary M, et al Effect of weave type variation on tensile and tearing strength of woven fabric
99. Parsons EM, Weerasooriya T, Sarva S, Socrate S (2010) Impact of woven fabric: experiments and mesostructure-based continuum-level simulations. J Mech Phys Solids 58:1995–2021. https://doi.org/10.1016/j.jmps.2010.05.006
100. Zhou Y, Chen X, Wells G (2014) Influence of yarn gripping on the ballistic performance of woven fabrics from ultra-high molecular weight polyethylene fibre. Compos B Eng 62:198–204. https://doi.org/10.1016/j.compositesb.2014.02.022
101. Tan VBC, Tay TE, Teo WK (2005) Strengthening fabric armour with silica colloidal suspensions. Int J Solids Struct 42:1561–1576. https://doi.org/10.1016/j.ijsolstr.2004.08.013
102. Das A (2012) Testing and statistical quality control in textile manufacturing. In: Process Control in Textile Manufacturing. Elsevier Ltd, pp 41–78
103. Süle G (2012) Investigation of bending and drape properties of woven fabrics and the effects of fabric constructional parameters and warp tension on these properties. Text Res J 82:810–819. https://doi.org/10.1177/0040517511433152